

MIDAS: Multi-agent Interaction-aware Decision-making with Adaptive Strategies for Urban Autonomous Navigation

Xiaoyi Chen

Nuro, Inc.*

xiaoyich@alumni.upenn.edu

Pratik Chaudhari

Department of Electrical and Systems Engineering,

University of Pennsylvania.

pratikac@seas.upenn.edu

Abstract: Autonomous navigation in crowded, complex urban environments requires interacting with other agents on the road. A common solution to this problem is to use a prediction model to guess the likely future actions of other agents. While this is reasonable, it leads to overly conservative plans because it does not explicitly model the mutual influence of the actions of interacting agents. This paper builds a reinforcement learning-based method named MIDAS where an ego-agent learns to affect the control actions of other cars in urban driving scenarios. MIDAS uses an attention-mechanism to handle an arbitrary number of other agents and includes a “driver-type” parameter to learn a single policy that works across different planning objectives. We build a simulation environment that enables diverse interaction experiments with a large number of agents and methods for quantitatively studying the safety, efficiency, and interaction among vehicles. MIDAS is validated using extensive experiments and we show that it (i) can work across different road geometries, (ii) results in an adaptive ego policy that can be tuned easily to satisfy performance criteria such as aggressive or cautious driving, (iii) is robust to changes in the driving policies of external agents, and (iv) is more efficient and safer than existing approaches to interaction-aware decision-making.

1 Introduction

Consider an autonomous vehicle (henceforth called the “ego”) that is turning left at an intersection: when sharing the road with other vehicles, a typical planning algorithm would predict the forward motion of the other cars and ego would stop until it is deemed safe and legal to proceed. This is a reasonable approach for situations where the right-of-way is clear. It is however quite inefficient when the right-of-way is unclear, ego is overly conservative [1], or when human-driven vehicles exploit a conservative ego policy¹. We may mitigate this inefficiency by enabling communication between the vehicles. Perhaps the most natural form of communication comes from mimicking the typical human behavior of inching forward towards the intersection to make their intent known to others; this is powerful because it does not require additional infrastructure and enables other human drivers to reason about autonomous vehicles the same way they would reason about any other human-driven vehicle. This paper devises such driving strategies for autonomous vehicles that can influence the actions of other drivers, specifically other human drivers.

The challenges to solving the above problem and our contributions to mitigating them are as follows.

1. **Driving safely and efficiently is hard because the intent of the other drivers is unknown.** We model the interaction problem as a partially-observable Markov decision process where the ego agent only observes the states of other agents in its vicinity and maximizes a reward that encourages it to reach a goal region in minimal time while avoiding collisions. Non-ego agents drive using an Oracle policy that has full access to trajectories of nearby agents. A “driver-type” variable, which is not observable to others, allows the user to tune the policy to be aggressive or cautious.
2. **Ability to handle an arbitrary number of agents, who may not affect the optimal action.** We parametrize the ego policy using an attention-based architecture which can

*Work done while at the University of Pennsylvania.

¹ The View from the Front Seat of the Google Self-Driving Car

handle an unordered, arbitrary number of agents in the observation range. Attention allows the ego policy to only focus on agents that are relevant to decision making. In contrast, most current literature studies interaction among a fixed [2] or limited number of agents [3, 4].

3. **Learning interaction policies without knowing the dynamics of external agents.** We use off-policy reinforcement learning (RL) methods to learn the policy and include two variations of typical implementations which reduce the variance of the action selection and stabilize the target function in temporal-difference learning.
4. **A platform for extensive and systematic interaction experiments.** We build a simulation environment that enables carefully designed interaction experiments with a large number of agents in diverse road geometries such as turns, T-intersections, and roundabouts. We devise a number of metrics that allow fine-grained reporting of safety and efficiency of ego’s policy. We can quantitatively study how ego influences the actions of external agents in this environment. We perform extensive experiments in realistic scenarios to show that MIDAS (i) can work across different road geometries, (ii) results in an adaptive ego policy that can be tuned easily to satisfy performance criteria such as aggressive or cautious driving, (iii) is robust to changes in the driving policies of external agents, and (iv) is more efficient and safe than existing approaches to interaction-aware decision-making.

2 Problem Formulation

Consider n agents with the state of the k^{th} vehicle at time $t \in \mathbb{Z}_{\geq 0}$ denoted by $x_t^k \in \mathbb{R}^d$. Denote the combined state of all agents by $x_t^{\text{all}} := [x_t^1, \dots, x_t^n]$. The control input for the k^{th} agent and the control input of the combined system are denoted by u_t^k and $u_t^{\text{all}} = [u_t^1, \dots, u_t^n]$ respectively. We will consider a deterministic discrete-time system $x_{t+1}^{\text{all}} = f(x_t^{\text{all}}, u_t^{\text{all}})$; $x_0^{\text{all}} \sim p_0$ where the initial state x_0^{all} is drawn from a distribution p_0 . The ego agent has index 1 and to keep the exposition clear, we will simply denote its state, control and driver-type by x_t, u_t and β respectively. The notation x_t^{-e} and β^{-e} refer to the combined state and driver-type of all agents other than ego.

Driver-type and observation model. Each agent possesses a real-valued parameter $\beta^k \in [-1, 1]$ that models its “driver-type”. A large value of β^k indicates an aggressive agent and a small value of β^k indicates that the agent is inclined to wait for others around it before making progress. The crux of our problem formulation is that an agent cannot observe the driver-type of the other agents. At each time t , each agent k has access to observations $o_t^k = \{x_t^i : d(x_t^k, x_t^i) \leq D, i = 1, \dots, n\}$ that consist of the states of all agents (including k) within some distance D . This model is a multi-agent Partially-Observable Markov Decision Process (POMDP): agents do not have access to the entire state of the problem due to a limited observation range, and they cannot observe the driver-type of others. Agents-specific goal locations x_g^k are sampled randomly using a goal distribution p_g . The reward function $r^k(x_t^{\text{all}}; x_g^k, \beta^k)$ encourages agents to reach their goal location in minimal time while avoiding collisions with other agents. It encourages different behavior based on β^k . Ego’s goal state is denoted by x_g . Collision is defined as two agents coming within some distance $\delta_{\text{collision}}$ of each other, assuming a uniform rectangular geometry for all agents. The deterministic control policy for each agent is $\pi^k(o_t^k; \beta^k)$. Given policies of the other agents π^{-e} , ego maximizes the objective

$$\mathbb{E}_{x_0^{\text{all}} \sim p_0, x_g^{\text{all}} \sim p_g, \beta^{-e}} \left[\sum_{t=0}^{\infty} \gamma^t r(x_t^{\text{all}}; x_g, \beta) \mid x_{t+1} = f(x_t, u_t), u_t = \pi(o_t; \beta), x_g, x_0, \pi^{-e} \right]. \quad (1)$$

to obtain a policy $\pi^*(\beta)$ which is a function of its driver-type β . Ego’s policy can thus be easily evaluated for a different value of β . The constant $\gamma < 1$ is a discount factor.

Simplifications. We are interested in $n \in [0, 25]$ agents and the problem formulation above is a large decentralized POMDP which is known to be intractable [5]. We make the following simplifications.

- (i) We include waypoints as a part of the observation of vector o_t^k . This enables the policy π^k to focus the learning only on handling the interactions instead of spending sample complexity and model capacity on learning motion-planning behaviors. A shortest-path algorithm that finds the trajectory from the agent state x_t^k to its goal state x_g^k *without considering other agents on the road as obstacles* is used to compute these waypoints.
- (ii) Control actions of all agents are $u_t^k \in \{0, 1\}$ which correspond to stop and go respectively.
- (iii) All non-ego agents use the same policy π^{-e} . This policy, called the Oracle, is fixed to a user-designed policy (details in Sec. 4.1) and serves as a benchmark for learned policies.

These simplifications reduce our problem formulation to that of a standard POMDP, albeit with unknown dynamics, where only ego’s policy is learned.

3 The MIDAS Approach

3.1 Off-policy Training

Define the action-value function

$$q(o, u; \beta) = \mathbb{E}_{x_g^{\text{all}} \sim p_g, \beta^{-e}} \left[\sum_{t=0}^{\infty} \gamma^t r(x_t^{\text{all}}; x_g, \beta) \mid x_0 = x, u_0 = u, u_t = \pi(o_t; \beta) \right] \quad (2)$$

as the expected reward obtained using the policy π after starting from the initial state x and control u . Off-policy methods are a popular technique to estimate this value function and learn the optimal policy by minimizing the Bellman error, also called the 1-step temporal difference (TD) error,

$$\text{TD} := q(o_t, u_t) - r(x_t^{\text{all}}; x_g, \beta) - \gamma q(o_{t+1}, \pi(o_{t+1}; \beta)) \quad (3)$$

over a dataset $\mathcal{D} = \{(o_t, u_t, r_t, o_{t+1})\}_{t=0, \dots}$, that is collected using a (behavior) policy that may be different from π . If the value function q_θ is parameterized using a function approximator, say a deep neural network with parameters θ , the TD-error is a function of these parameters θ . Further, if the control-space is discrete (as is the case for us) we can set $\pi(o_t; \beta) := \text{argmax}_{u'} q_\theta(o_t, u')$ and learn the optimal value function by performing stochastic gradient descent to solve

$$\theta^* = \text{argmin}_\theta \frac{1}{|\mathcal{D}|} \sum_{(o_t, u_t, r_t, o_{t+1}) \in \mathcal{D}} \text{TD}^2(\theta). \quad (4)$$

This objective can be seen as the regression error of the first term $q_\theta(o_t, u_t)$ in (3) against the sum of the other two terms which are together called the *target*. This objective forms the basis for the well-known DQN algorithm [6]. Off-policy methods are superior to others such as policy-gradient methods because they reuse the dataset \mathcal{D} multiple times while learning q_θ . However, implementing them successfully in practice comes with a few caveats which we describe next.

Tricks of the trade in off-policy RL. The TD² objective in (4) can be zero even if the value function is not accurate because the Bellman operator is only a contraction in the ℓ_∞ norm, not the ℓ_2 norm [7]. This leads to instabilities during training which are mitigated by a number of tricks that replace the value function $q_\theta(o_{t+1}, \text{argmax}_{u'} q_\theta(o_{t+1}, u'))$ used in (3). A popular scheme is to use time-lagged version of the parameters, i.e., use $\max_{u'} q_{\theta_{\text{lag}}}(o_{t+1}, u')$ [6]. Over-estimation bias of the value function estimate [8] is countered by using two (or more) copies of the parameters $\{q_{\theta^i}, i = 1, 2\}$ along with time-lagged versions for both and using the minimum of these two $\min_{i=1,2} \{q_{\theta_{\text{lag}}^i}(o_{t+1}, \text{argmax}_{u'} q_{\theta_{\text{lag}}^i}(o_{t+1}, u'))\}$ to compute the target. Parameters of both copies are updated using the objective in (4). A variant of this is Double Q Learning [9] which uses $q_{\theta_{\text{lag}}}(o_{t+1}, \text{argmax}_{u'} q_\theta(o_{t+1}, u'))$. Notice that the target is computed using the time-lagged parameters but action is computed using the *current, non-lagged* parameters. This ensures a fair evaluation of the value of the greedy policy given by the *current* parameters.

Our improvements to off-policy RL. The above techniques are typically combined together in state-of-the-art off-policy algorithms. We introduce two variants which further improve the stability of training. First is to mix the two parameter copies when using the Double Q Learning trick:

$$q_\theta(o_{t+1}, \text{argmax}_{u'} q_\theta(o_{t+1}, u')) := \min_{i,j \in \{1,2\}, i \neq j} \left\{ q_{\theta_{\text{lag}}^i}(o_{t+1}, \text{argmax}_{u'} q_{\theta^j}(o_{t+1}, u')) \right\}. \quad (5)$$

This forces the first copy, via its time-lagged parameters to be the evaluator for the second copy and vice-versa; it leads to further variance reduction of the target in the TD objective. A second variation we use is to pick the action during *policy evaluation* using the average of the two copies

$$\pi(o_t; \beta) = \text{argmax}_{u'} \frac{1}{2} \sum_{i=1}^2 q_{\theta^i}(o_t, u'). \quad (6)$$

Observe that doing so does not invalidate the Bellman equation: if both the value function estimates are optimal, the action predicted by their average is also optimal. The average reduces the variance of picking the best action. These variations can be implemented with less than 10 lines of code in state-of-the-art off-policy RL algorithms and only change the computational cost marginally.

3.2 Attention-based Policy Architecture

Our value function should be *permutation invariant*: ordering of the states in the observation vector α_t should not affect ego’s action. It should also be able to *handle an arbitrary number of other agents*. The optimal action only depends on the *actionable information* [10], namely agents whose states cause a change in ego’s action. We next discuss an architecture that bakes in these properties.

Permutation-invariant input representation. [11] shows that a function $\phi(A)$ operating on a set A is invariant to permutation of the elements in A iff it can be decomposed as $\phi(A) \equiv \rho(\sum_{a \in A} \varphi(a))$ for some functions φ and ρ . This is a remarkable result because both φ, ρ can now be learnt to build invariance. The summation (average pooling) enables $\phi(A)$ to handle sets with varying number of elements. Observe however that the summation assigns the same weight to all elements in the input. As we see in our experiments, a value function using this “DeepSet” architecture is likely to be distracted by agents that do not inform the optimal action.

Attention. An attention mechanism [12] takes in elements of the set A and outputs a linear combination $z(a) = \sum_{a' \in A} \alpha_{a,a'} \varphi_v(a')$ where $\varphi_v(a)$ is the “value” embedding of a and weights $\alpha_{a,a'} = \langle \varphi(a), \varphi(a') \rangle$ compute the similarity of different elements. A generalization of this is the attention module of [12] which uses $\alpha_{a,a'} = \langle \varphi_k(a), \varphi_q(a') \rangle$. Similarity is thus computed across a set of “keys” φ_k and a set of “queries” φ_q , all of which are learned. An attention module is an elegant way for the value function to learn key, query, value embeddings that pay more attention to parts of the input that are more relevant to the output. E.g, [13] sets the key to be an encoding of ego’s state, which is compared to query and value embeddings generated from the observation vector.

Set-based attention [14] in MIDAS. The summation in attention throws away higher-order correlations since φ_v is computed independently for each a . A better representation for set-valued inputs can be created using: (i) a *set-attention block* (SAB) (we use its efficient version *induced* SAB) which builds $\varphi_v(a)$ itself using self-attention; (ii) another self-attention mechanism to aggregate features instead of simple summation; this is called *pooling by multi-head attention* (PMA), (iii) regularization techniques such as layer-normalization [15] and residual connections [16], and (iv) *multi-head attention* [12] that computes inner products independently across subspaces of the embedding.

Encoding ego’s driver-type. We want ego’s driver-type information to only affect the encoding of its own state, not the state of the other agents, in the observation vector; this is akin to masking NLP [17]. We use a two-layer perceptron with ReLU nonlinearities to embed the scalar variable β and add the output to the encoding of ego’s state.

3.3 Designing the reward function

The reward function for ego in our problem is designed to encourage it to make progress towards its x_g while minimizing the time taken and the collisions with the other agents on the road. It consists of a time-penalty for every timestep, reward for non-zero speed, timeout penalty that discourages ego from stopping the traffic flow (this includes a stalemate penalty where all nearby agents including ego are standstill waiting for one of them to take initiative and break the tie), a collision penalty and a penalty for following too close to the agent in front. All these sub-rewards except the last one depend linearly on β ; they have the form $w\beta + b$ where the weight w and the bias b are chosen (see Appendix A.2) to achieve good performance on downstream metrics such as time-to-finish, collision, timeout and success rates *using a generic RL agent*. We emphasize that designing ego’s reward this way is reasonable and indeed what an algorithm designer will do in practice [18].

4 Experiments

4.1 Evaluation Methodology

The outcome of a multi-agent planning problem under partial observations is inherently noisy. It is therefore important to build an evaluation suite which provides fine-grained understanding but also allows studying complex scenarios.

Simulation environment. Fig. 1 shows our simulation environment which consists of 4 T-intersections, 4 corners and a roundabout. Lanes with direction information are encoded into the map. An episode begins with each agent initialized at a random location and with a randomly chosen goal location. Each agent is randomly assigned a driver type $\beta \in [-1, 1]$: the driver-type

determines the agent’s velocity as $v = 2.7\beta + 8.3$; these constants are based on the recommended turning velocity of the turning radii in the environment [19]. A timestep in the environment is 0.1s. For Oracle agents (see below), the observation vector contains the states of all agents within a travel-distance of 9.2m along their paths. Non-Oracle agents do not have global information about other agents’ path information. Their observation vector contains the locations of all agents within a *Euclidean* distance of 10m and is created in an ego-centric coordinate frame; this is a simple technique to make the policy generalize trivially to new maps without further training.

Oracle planner. Non-ego agents run an Oracle planner which is executed as follows. For any two agents $i, j, i \neq j$ let $\tau_{0,1}^{ij}$ be the time-to-collision (TTC) if agent i takes action zero (stops) for all time-steps henceforth and agent j moves forward along its waypoints for all time-steps henceforth. The TTC can be infinite. At every timestep, the Oracle planner of i compares $\tau_{0,1}^{ij}$ with $\tau_{1,0}^{ij}$ for all agents j within its observation range and stops if the former is larger. A tie between the two values is broken by giving priority to $\min(i, j)$, but any other mechanism can be used here.

Systematically creating an evaluation dataset. We curate (i) *generic episodes* that consist of a random number of agents with uniformly random initial and goal locations, (ii) *collision episodes* which ensure that the ego will collide with at least one other agent in the future if it does not stop at an appropriate timestep, and (iii) *interaction episodes* which ensure that 2–3 agents (including ego) arrive at a location simultaneously (or within 4 timesteps of each other so as to trigger our collision threshold). Interaction episodes are illustrated in Appendix B.1. Ego cannot do well in interaction episodes unless it negotiates with other agents. We randomize over the number of agents, driver-types, agent IDs, road geometries, and add small perturbations to their arrival time to construct 1917 interaction episodes. We use a mix of the three kinds of episodes during training and use a mix of generic and interaction episodes, reflective of general driving settings with an emphasis on interactions, for validation and testing. We separately report the test performance of interactive episodes. See Appendix B.2 for more details. Curating the dataset in this fashion aids the reproducibility of results compared to using random seeds to initialize the environment, as is commonly done.

Evaluation Metrics. We evaluate performance based on (i) the *time-to-finish* which is the average episode length, and (ii) *collision, timeout and success rate* which refer to the percentage of episodes that end with the corresponding status (the three add up to 1). To qualitatively compare performance, we prioritize collision rate (an indicator for safety) over the timeout rate and time-to-finish (which indicate efficiency). Performance of the Oracle planner is reported over 4 trials; performance of the trained policy is reported across 4 random seeds.

Baselines. We perform comprehensive benchmarking and compare MIDAS against the Oracle planner which is the gold-standard and acts as an upper bound on performance, a simple *Car Follower* that keeps a fixed minimum distance from the agent in front which acts as a lower bound on performance, and learning-based models such as a multi-layer perceptron (MLP), Deep Set [11] which is a popular architecture for prediction models [20], and Social Attention [13] to fit the value function. Appendix C provides more implementation details.

4.2 Results

Table 1 reports test performance of all algorithms across three different metrics on the test set and the test interaction set. Box plots in Fig. 2 show the same information; training curves are given in Appendix D.1. We next discuss these results in the context of specific questions.

1. Is the learned model safe and efficient? First, our experiments show that learning interactive driving policies is indeed beneficial: MLP and MIDAS both achieve lower collision rates than the rule-based Car-Follower in both general driving (Fig. 2a) and interactive driving (Fig. 2b) settings. MIDAS is safer than the naive rule-based Car-Follower and other attention-based models while being as efficient as the Oracle. MIDAS has lower collision rate than all other learned models. We also achieve the lowest timeout rates among all learned models. In terms of time-to-finish (Fig. 2c, Fig. 2d), it is remarkable that MIDAS is similar to Oracle even though the former does not have all the information (long-time horizon, tie-breaking priority) that the Oracle has access to.

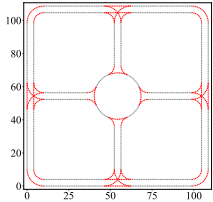


Figure 1: **Map of the environment**

Table 1: **Summary of empirical results.** Time-to-finish is average episode length within the set. Collision, timeout and success rates refer to the percentage of episodes within the set that end with the respective status. Lower collision rate indicates higher safety. Lower timeout rate and time-to-finish indicate higher efficiency. Higher success rate is better. We verified that most timeout cases for MIDAS are caused by ego stepping into the TTC thresholds of other agents and then stopping for other agents, while other Oracle-driven agents also choose to wait for ego, leading to a stalemate. In reality, stalemates like this are unlikely to happen because once ego stops, the other drivers would likely move forward and break the tie.

Planner	Test Set				Test Interaction Set			
	Time-to-finish	Collision (%)	Timeout (%)	Success (%)	Time-to-finish	Collision (%)	Timeout (%)	Success (%)
Oracle	66.57 ± 0.23	0.35 ± 0.17	0.10 ± 0.10	99.55 ± 0.17	72.68 ± 0.27	0.66 ± 0.13	0.20 ± 0.22	99.14 ± 0.11
Car Follower	61.20 ± 0.32	3.90 ± 0.54	0.00 ± 0.00	96.10 ± 0.54	64.91 ± 0.51	8.16 ± 1.22	0.00 ± 0.00	91.84 ± 1.22
MLP	66.78 ± 2.85	2.82 ± 1.25	1.56 ± 1.47	95.61 ± 2.52	71.88 ± 3.30	5.72 ± 1.69	2.30 ± 1.95	91.97 ± 2.62
DeepSet [11]	64.52 ± 2.04	4.59 ± 1.37	1.51 ± 1.13	93.90 ± 1.37	69.97 ± 3.35	7.83 ± 1.81	2.57 ± 1.78	89.61 ± 1.15
SocialAttention [13]	65.27 ± 5.06	6.45 ± 5.59	1.86 ± 1.48	91.68 ± 4.36	70.27 ± 5.21	7.17 ± 4.75	2.04 ± 1.41	90.79 ± 3.53
MIDAS (Ours)	68.61 ± 0.92	1.26 ± 0.66	0.45 ± 0.22	98.29 ± 0.54	72.34 ± 0.74	2.70 ± 1.14	0.46 ± 0.22	96.84 ± 1.05

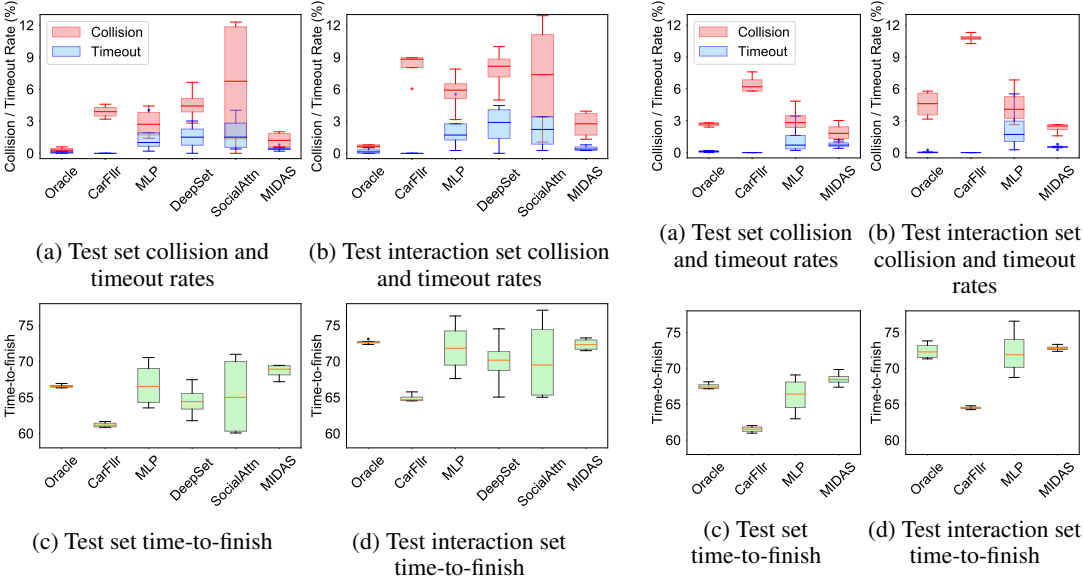


Figure 2: **MIDAS is safer than Car-Follower and other learned planners and similar to Oracle in efficiency.** Time-to-finish is average episode length within the set. Collision, timeout rates refer to the percentage of episodes that end with the respective status. CarFllr, SocialAttn refer to Car-Follower and Social Attention, respectively.

Figure 3: **MIDAS is more generalizable across different driving policies for the other agents.** Test performance with action noise for external agents. Oracle and Car-Follower collision rates greatly increase from those in Fig. 2 while the performance of MLP and MIDAS is unchanged.

2. Can the model generalize across different driving policies for the other agents? At test time, we add Bernoulli noise of probability 0.1 to the actions of other agents to model the fact that driving policies of other agents may be different from each other, and different from our gold-standard Oracle. As shown in Fig. 3, the Oracle’s collision rate is now larger, which can be directly attributed to conflicting actions taken by the agents during interaction. The rule-based Car-Follower *becomes* more aggressive in this case and although its time-to-finish is small, the collision rates are quite high. MLP performs about as well as the Oracle. In contrast to these, MIDAS has similar collision/timeout rates and time-to-finish from Fig. 2 and outperforms Oracle in both driving settings (Fig. 3). This shows that MIDAS can generalize better to different driving policies of other agents on the road.

3. Does MIDAS influence the actions of other agents? We curate test episodes where ego and one other agent arrive simultaneously at a given location if they take their nominal actions. The arrival time of the other agent is then perturbed to study how MIDAS changes its actions. The X-axis in Fig. 4 is the time period (in seconds) by which the other agent *precedes* ego. The Y-axis shows the percentage of timesteps where $u_t = 1$, i.e., ego drives forward. The size of the agents is such that if the arrival times are within 0.3s of each other, either ego or the other agent could go first. We see that ego takes the initiative in more than 94% of the cases if it arrives earlier than 0.3s (yellow region), where the right-of-way is ambiguous. Ego is likely to stop if the other agent arrives earlier

(red region). If the other agent arrives earlier by more than 1.5s (green region), the intersection is clear for the ego and the likelihood of proceeding forward goes back up. This experiment shows that in ambiguous situations, ego attempts to drive forward, just like a human driver would in the absence of right-of-way rules. At the same time, ego does stop if a collision is more likely.

Next we study ego’s behavior in safety-critical situations. Fig. 5 compares the percentage of timesteps where ego goes forward (Y-axis) against the minimum TTC across all agents in the vicinity if both ego and the other agent decide to go forward (X-axis). For small TTC when collision is immediate, MIDAS is less likely to proceed than MLP. This shows that MIDAS does not blindly drive forward in safety critical situations.

4. Does the model make decisions properly in highly interactive situations? We define highly interactive situations for agent i as those where $\tau_{1,0}^{ij}$ (green line in Fig. 6b, Fig. 6d) is lower than a threshold, indicating that there’s at least one other agent very close by which forces i to stop. We run Oracle on the test set and *record what the learned model would have done if it were in the same situation* as the Oracle. In car-following (Fig. 6a), Oracle stops for the front vehicle a long distance away while blocking the traffic at an intersection, but MIDAS chooses to move forward and stop closer to the front vehicle. In left-turn (Fig. 6c), Oracle waits until there’s a big clearance after agent 1 turns right before proceeding, but MIDAS drives forward right after. Both episodes show how MIDAS drives more efficiently. Refer to Appendix D.2 for illustrations.

5. Are MIDAS’ strategies adaptive? How does model performance change with driver-type? At test time, we change the ego driver type to $-1, -0.5, 0, 0.5, 1$ and run it on the test set with all other agents running the Oracle planner. The results are shown in Fig. 7. MIDAS plans more efficiently as ego driver type increases, as shown in the decreasing time-to-finish (Fig. 7b), while maintaining the collision rate almost constant (Fig. 7a). Fig. 7a also shows that MIDAS is consistently safer than all other learned models across different ego driver types. MIDAS timeout rate is relatively constant across ego driver types and is shown in Appendix D.3.

6. MIDAS performs consistently across different driving scenes. Fig. 7c shows that the collision rate of MIDAS is consistently lower than other models. The collision/timeout rates also show only a small variation across intersection types.

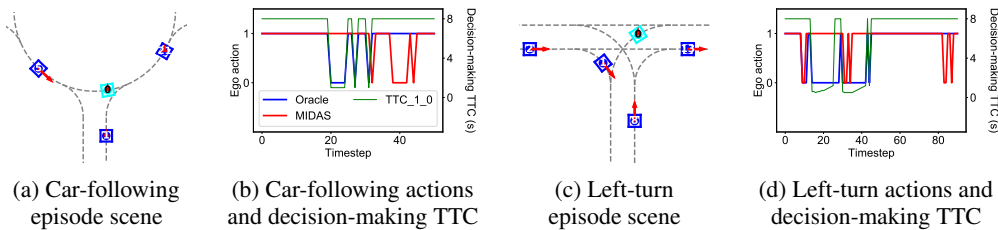


Figure 6: **Typical episodes where MIDAS differs from Oracle.** Ego is cyan; all other agents are blue. In car-following, Oracle stops for front vehicle at a far distance while blocking traffic at an intersection, but MIDAS chooses to stop later. In left-turn, Oracle waits until there’s a big clearance after agent 1 turns right before proceeding, but MIDAS drives forward right after. Both episodes illustrate how MIDAS drives more efficiently. Plots show Oracle (blue) actions, MIDAS (red) actions and $\tau_{1,0}^{1j}$ (green).

5 Related Work

Intention-aware planning with known dynamics for agents can be formulated as a POMDP, see e.g., [21] and solved using point-based solvers [22]. The focus is typically on planning a safe trajectory and not on interaction [23]. For urban driving, one may assume knowledge of road safety

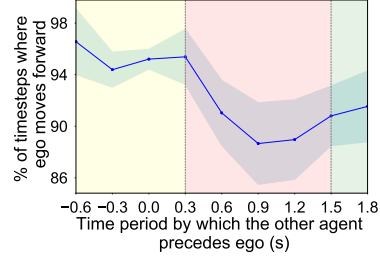


Figure 4: In ambiguous situations without clear right-of-way (yellow) or if the intersection clears before ego arrives (green), MIDAS drives forward. But it stops more often if a collision is more likely (red).

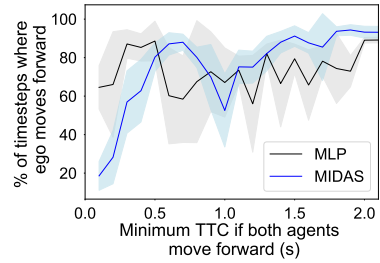


Figure 5: For small TTC when collision is immediate, MIDAS is less likely to proceed than MLP, indicating that MIDAS does not blindly drive forward in safety critical situations.

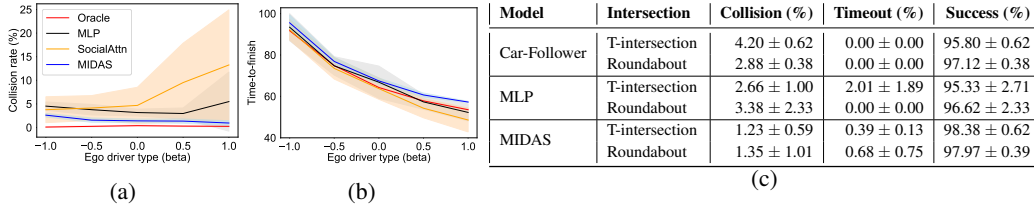


Figure 7: **MIDAS’ strategy is adaptive.** Figs. 7a and 7b shows that MIDAS plans more efficiently and is consistently safer than all other learned models as ego driver type changes. Deep Set and Car-Follower both perform worse than MIDAS and are not shown here for clarity. SocialAttn refers to SocialAttention. Fig. 7c shows test performance of Car-Follower, MLP and MIDAS at different intersections.

rules and use game-theoretic formulations to model multi-agent decision making [24, 25]. Interactive, model-free highway driving using deep RL is popular, e.g., policies for dense traffic using a prediction model [26], or ones that incorporate actions of other agents [3]. These papers involve fewer and easier interactions than ours. Merging has been studied in [2, 27] using predictive models for model predictive control, estimating future horizon cost via exhaustive search or Monte-Carlo rollout. MIDAS is complementary to these approaches and although we do not use a prediction model to narrow down our focus to interactions, such a model can be easily incorporated using model-based RL techniques.

Our use of adjustable driver type is similar to [18] where aggressive agents are encouraged to merge faster by overtaking others. This work however uses self-play to train the policy and while this approach is reasonable for highway merging, the competition is likely to result in high collision rates in busy urban intersections such as ours.

[28] uses inverse RL to learn the cost function of human drivers and uses it to influence other drivers. This method is computationally expensive and is limited to simplistic interactions. One may improve this by separating long-term and near-time planning at the cost of optimality [29]. In comparison, our attention-based model can scale to interaction with a large number of agents; our quantitative evaluation methods are also more thorough.

Learning-based approaches use featurization to tackle different lane geometries [4], roundabouts [30], or use simplified sequential action representations [31]. The observation vector is a concatenation of the states of other agents [2], spatial pooling that aggregates past trajectories of each agent [20], or birds-eye-view rasterization [32, 33]. In contrast, the set-transformer in MIDAS is an easy, automatic way to encode variable-sized observation vectors. In this sense, our work is closest to “Social Attention” in [13] which learns to influence other agents based on road priority and demonstrates results on a limited set of road geometries; MIDAS compares favorably to this method in Sec. 4.

6 Discussion

We studied interactions of autonomous vehicles with other vehicles in urban driving scenarios. We used deep RL techniques to learn a policy for an autonomous agent that can influence the actions of other agents. Interaction-aware autonomous driving is a pertinent problem but it is difficult to analyze systematically across different scenarios. Our work is a step towards improving the status quo. Its key features are user-tunable adaptive policies that are trained efficiently, the ability to pay attention to only the part of the observation vector that matters for control irrespective of the number of other agents in the vicinity, and an evaluation methodology that can answer difficult questions like “does the ego agent influence other agents”, or “how does the agent perform in highly interactive settings” in a quantitative and systematic manner.

Our goal is to translate interaction-aware planning from simulation to reality. On the algorithmic side, the main challenge is to build intent-aware prediction models and perform probabilistic reasoning over their outcomes while building the policy. As far as an implementation on autonomous vehicles is concerned, we are cognizant of the fact that deep RL policies have a very high variance in their real-world performance. Indeed, any learning-based approach is essentially blind to behaviors *not* present in the data. Our work should be thought of as providing a prior—that can be tuned via the driver-type to be more optimistic than a worst-case assumption—for existing planning algorithms for autonomous driving that build upon rapidly-exploring random trees [34, 35], model predictive control [36] etc.

References

- [1] P. Trautman, J. Ma, R. M. Murray, and A. Krause. Robot navigation in dense human crowds: Statistical models and experimental studies of human–robot cooperation. *The International Journal of Robotics Research*, 34(3):335–356, 2015.
- [2] E. Schmerling, K. Leung, W. Vollprecht, and M. Pavone. Multimodal probabilistic model-based planning for human-robot interaction. In *2018 IEEE International Conference on Robotics and Automation (ICRA)*, pages 1–9. IEEE, 2018.
- [3] N. Rhinehart, R. McAllister, K. Kitani, and S. Levine. Precog: Prediction conditioned on goals in visual multi-agent settings. In *Proceedings of the IEEE International Conference on Computer Vision*, pages 2821–2830, 2019.
- [4] C. Li and K. Czarnecki. Urban driving with multi-objective deep reinforcement learning. In *Proceedings of the 18th International Conference on Autonomous Agents and MultiAgent Systems*, pages 359–367. International Foundation for Autonomous Agents and Multiagent Systems, 2019.
- [5] F. A. Oliehoek, C. Amato, et al. *A concise introduction to decentralized POMDPs*, volume 1. Springer, 2016.
- [6] V. Mnih, K. Kavukcuoglu, D. Silver, A. A. Rusu, J. Veness, M. G. Bellemare, A. Graves, M. Riedmiller, A. K. Fidjeland, G. Ostrovski, et al. Human-level control through deep reinforcement learning. *Nature*, 518(7540):529–533, 2015.
- [7] D. P. Bertsekas. Weighted sup-norm contractions in dynamic programming: A review and some new applications. *Dept. Elect. Eng. Comput. Sci., Massachusetts Inst. Technol., Cambridge, MA, USA, Tech. Rep. LIDS-P-2884*, 2012.
- [8] R. S. Sutton and A. G. Barto. *Reinforcement learning: An introduction*. MIT press, 2018.
- [9] H. V. Hasselt. Double q-learning. In *Advances in neural information processing systems*, pages 2613–2621, 2010.
- [10] S. Soatto. Actionable information in vision. In *Machine learning for computer vision*, pages 17–48. Springer, 2013.
- [11] M. Zaheer, S. Kottur, S. Ravanbakhsh, B. Póczos, R. R. Salakhutdinov, and A. J. Smola. Deep sets. In *Advances in neural information processing systems*, pages 3391–3401, 2017.
- [12] A. Vaswani, N. Shazeer, N. Parmar, J. Uszkoreit, L. Jones, A. N. Gomez, L. Kaiser, and I. Polosukhin. Attention is all you need. In *NIPS*, 2017.
- [13] E. Leurent and J. Mercat. Social attention for autonomous decision-making in dense traffic. *arXiv preprint arXiv:1911.12250*, 2019.
- [14] J. Lee, Y. Lee, J. Kim, A. R. Kosiorek, S. Choi, and Y. W. Teh. Set transformer: A framework for attention-based permutation-invariant neural networks. *arXiv preprint arXiv:1810.00825*, 2018.
- [15] J. L. Ba, J. R. Kiros, and G. E. Hinton. Layer normalization. *arXiv preprint arXiv:1607.06450*, 2016.
- [16] K. He, X. Zhang, S. Ren, and J. Sun. Identity mappings in deep residual networks. In *European conference on computer vision*, pages 630–645. Springer, 2016.
- [17] J. Devlin, M.-W. Chang, K. Lee, and K. Toutanova. Bert: Pre-training of deep bidirectional transformers for language understanding. *arXiv preprint arXiv:1810.04805*, 2018.
- [18] Y. Hu, A. Nakhaei, M. Tomizuka, and K. Fujimura. Interaction-aware decision making with adaptive strategies under merging scenarios. *arXiv preprint arXiv:1904.06025*, 2019.
- [19] M. W. Hancock and B. Wright. A policy on geometric design of highways and streets. *American Association of State Highway and Transportation Officials: Washington, DC, USA*, 2013.
- [20] A. Gupta, J. Johnson, L. Fei-Fei, S. Savarese, and A. Alahi. Social gan: Socially acceptable trajectories with generative adversarial networks. In *Proceedings of the IEEE Conference on Computer Vision and Pattern Recognition*, pages 2255–2264, 2018.
- [21] T. Bandyopadhyay, K. S. Won, E. Frazzoli, D. Hsu, W. S. Lee, and D. Rus. Intention-aware motion planning. In *Algorithmic foundations of robotics X*, pages 475–491. Springer, 2013.
- [22] H. Bai, S. Cai, N. Ye, D. Hsu, and W. S. Lee. Intention-aware online pomdp planning for autonomous driving in a crowd. In *2015 IEEE International Conference on Robotics and Automation (ICRA)*, pages 454–460. IEEE, 2015.
- [23] T. Wongpiromsarn, A. Ulusoy, C. Belta, E. Frazzoli, and D. Rus. Incremental temporal logic synthesis of control policies for robots interacting with dynamic agents. In *2012 IEEE/RSJ International Conference on Intelligent Robots and Systems*, pages 229–236. IEEE, 2012.

- [24] P. Chaudhari, T. Wongpiromsarny, and E. Frazzoli. Incremental minimum-violation control synthesis for robots interacting with external agents. In *2014 American Control Conference*, pages 1761–1768. IEEE, 2014.
- [25] M. Zhu, M. Otte, P. Chaudhari, and E. Frazzoli. Game theoretic controller synthesis for multi-robot motion planning part i: Trajectory based algorithms. In *2014 IEEE International Conference on Robotics and Automation (ICRA)*, pages 1646–1651. IEEE, 2014.
- [26] M. Henaff, A. Canziani, and Y. LeCun. Model-predictive policy learning with uncertainty regularization for driving in dense traffic. *arXiv preprint arXiv:1901.02705*, 2019.
- [27] S. Bae, D. Saxena, A. Nakhaei, C. Choi, K. Fujimura, and S. Moura. Cooperation-aware lane change maneuver in dense traffic based on model predictive control with recurrent neural network.
- [28] D. Sadigh, S. Sastry, S. A. Seshia, and A. D. Dragan. Planning for autonomous cars that leverage effects on human actions. *Robotics: Science and Systems*, 2016.
- [29] J. F. Fisac, E. Bronstein, E. Stefansson, D. Sadigh, S. S. Sastry, and A. D. Dragan. Hierarchical game-theoretic planning for autonomous vehicles. In *2019 International Conference on Robotics and Automation (ICRA)*, pages 9590–9596. IEEE, 2019.
- [30] J. Chen, B. Yuan, and M. Tomizuka. Model-free deep reinforcement learning for urban autonomous driving. In *2019 IEEE Intelligent Transportation Systems Conference (ITSC)*, pages 2765–2771. IEEE, 2019.
- [31] D. Isele, R. Rahimi, A. Cosgun, K. Subramanian, and K. Fujimura. Navigating occluded intersections with autonomous vehicles using deep reinforcement learning. In *2018 IEEE International Conference on Robotics and Automation (ICRA)*, pages 2034–2039. IEEE, 2018.
- [32] Y. Tang. Towards learning multi-agent negotiations via self-play. In *Proceedings of the IEEE International Conference on Computer Vision Workshops*, pages 0–0, 2019.
- [33] M. Bansal, A. Krizhevsky, and A. Ogale. Chauffeurnet: Learning to drive by imitating the best and synthesizing the worst. *arXiv preprint arXiv:1812.03079*, 2018.
- [34] Y. Kuwata, G. A. Fiore, J. Teo, E. Frazzoli, and J. P. How. Motion planning for urban driving using rrt. In *2008 IEEE/RSJ International Conference on Intelligent Robots and Systems*, pages 1681–1686. IEEE, 2008.
- [35] A. Censi, K. Slutsky, T. Wongpiromsarn, D. Yershov, S. Pendleton, J. Fu, and E. Frazzoli. Liability, ethics, and culture-aware behavior specification using rulebooks. In *2019 International Conference on Robotics and Automation (ICRA)*, pages 8536–8542. IEEE, 2019.
- [36] C. Urmson, J. Anhalt, D. Bagnell, C. Baker, R. Bittner, M. Clark, J. Dolan, D. Duggins, T. Galatali, C. Geyer, et al. Autonomous driving in urban environments: Boss and the urban challenge. *Journal of Field Robotics*, 25(8):425–466, 2008.

Supplementary Material

MIDAS: Multi-agent Interaction-aware Decision-making with Adaptive Strategies for Urban Autonomous Navigation

A Approach

A.1 Attention-based Policy Architecture

It’s important for the ego to be able to handle a varying number of other agents. We run one seed of MIDAS on the test set and plot the reward received per timestep against the agent density in ego’s vicinity, represented by the number of agents in ego’s observation range. Higher density indicates higher difficulty, because ego needs to pay attention to the more important agents. As shown in Fig. 8, MIDAS performance is consistent across situations with different difficulty. This suggests that the attention mechanism works well; it is able to pay attention to only relevant parts of the observation vector even when there is a large number of agents in the vicinity.

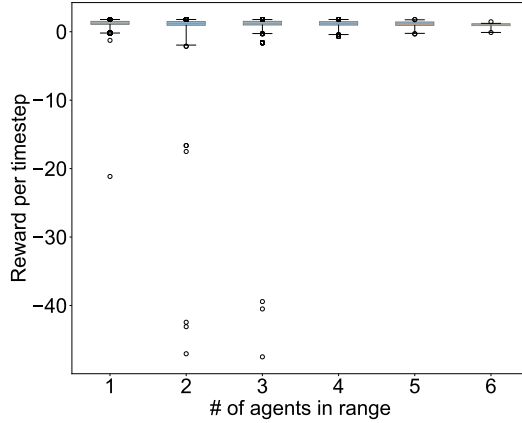


Figure 8: **MIDAS performance is consistent across situations with different difficulty.** Box plot of the reward *received* per timestep against agent density in ego’s vicinity. The box plot whiskers represent 0.5% and 99.5% percentiles.

A.2 Designing the Reward Function

The weights and biases of the reward function described in Sec. 3.3 are listed in (7). The adaptive cruise control penalty penalizes the agent for following too closely to the agent in front and is designed such that it’s capped between -2 and 0. The reward coefficients of all sub-rewards, except for stalemate penalty, are chosen using a generic RL agent, which has the same structure as MLP but does not use two copies of parameters. The agent was trained using the standard time-lagged Q-learning algorithm without the two variants introduced in Sec. 3.1. We added the stalemate penalty later to reduce the occurrence of timeouts across all models that were being trained.

$$r(x_t; x_g, \beta) = \begin{cases} -0.05\beta - 0.15 & \text{time penalty for every every timestep} \\ 0.5\beta + 1.5 & \text{if ego speed is non-zero} \\ -5\beta - 20 & \text{timeout penalty if } t = T_{\max} \\ -0.5\beta - 1.5 & \text{stalemate penalty} \\ -5\beta - 45 & \text{collision penalty} \\ -2 + \frac{2}{1+e^{-d_{\text{follow}}}} & \text{if ego within distance } \delta_{\text{follow}} \text{ of the car ahead of it} \end{cases} \quad (7)$$

B Evaluation Methodology

B.1 Types of Interaction Episodes

Fig. 9 shows the three basic types of interaction episodes described in Sec. 4.1.

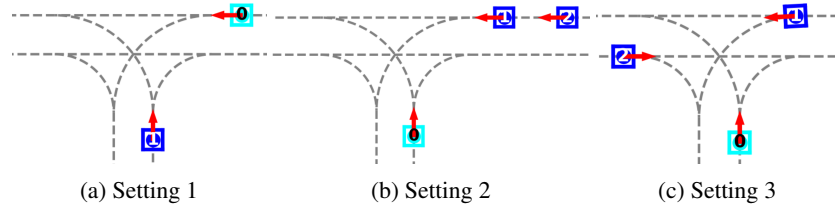


Figure 9: The interaction settings used for generating the interaction set. In Setting 1 and 2, agent 0 and 1 will simultaneously arrive at the lane intersection. In Setting 2, agent 2 is at the minimum following distance behind agent 1. In Setting 3, all three agents will arrive simultaneously at the lane intersection.

B.2 Training, Validation and Test Set Configurations

We use a mix of 25% generic episodes, 25% collision episodes, and 50% interaction episodes for training and a validation set composed of 100 random and 100 interaction episodes. For reporting the test performance, we use 250 generic episodes and 250 interaction episodes. This evaluation benchmark reflects general driving scenarios. We also use the test interaction set, which contains 381 interaction episodes, to evaluate model performance on interactive scenarios.

C Model Implementation Details

C.1 Model Architecture

The model architecture is shown in Fig. 10, and the detailed implementation of the models experimented with in Sec. 4 are shown in Table 2.

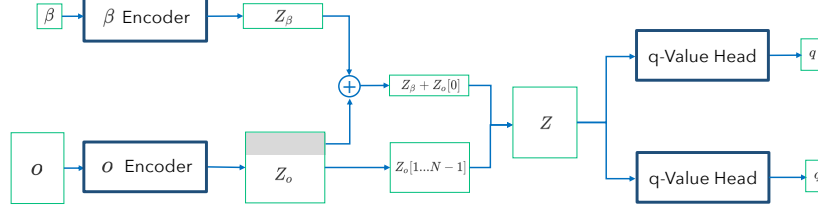


Figure 10: The architecture of MLP, DeepSet, SocialAttention and MIDAS. β , o refers to ego driver type and observation, respectively. The two values are encoded separately, and then the encoded β is added to the first row of the encoded o . After that, the encoding is passed into two q-value heads with identical structures, each outputting an estimate of the q-values of the two actions, mentioned in Sec. 3.1.

Table 2: Implementation of the components in the model shown in Fig. 10. The values in [] refer to input and output dimensions of fully-connected layers. $|o|$ refers to the dimension of the total state vector with all agent information, while $|o^k|$ refers to the dimension of the state vector of a single agent. ‘‘Int. Layer’’ refers to ‘‘Intermediate Layer’’, applied to the combined encoding Z in Fig. 10 before it’s passed into the two q-value heads. SocialAttention modules: Based on [13], the parameters in EgoAttention correspond to: hidden dimension, number of heads. MIDAS modules: Based on [14], the parameters in ISAB correspond to: input dimension, output dimension, number of heads, number of induced vectors, whether to apply LayerNorm (T/F); the parameters in PMA correspond to: input dimension, number of heads, number of seeds, whether to apply LayerNorm (T/F); the parameters in SAB correspond to: input dimension, output dimension, number of heads, whether to apply LayerNorm (T/F).

	MLP	DeepSet	SocialAttention	MIDAS
o Encoder	$[o ,128]$ ReLU $[128,128]$	$[o^k ,128]$ ReLU $[64,64]$ ReLU $[64,128]$	$[o^k ,64]$ ReLU $[64,64]$	ISAB($ o^k $, 128, 4, 32, T) ISAB(128, 128, 4, 32, T)
β Encoder	$[1,64]$ ReLU $[64,128]$	$[1,64]$ ReLU $[64,128]$	$[1,64]$ ReLU $[64,64]$ ReLU $[64,64]$	$[1,64]$ ReLU $[64,128]$ ReLU $[128,128]$
Int. Layer	/	$[128,128]$ ReLU $[128,128]$	$[64,64]$ ReLU $[64,64]$ EgoAttention(64,2)	/
q-Value Head	$[128,128]$ ReLU $[128,2]$	$[128,128]$ ReLU $[128,2]$	$[64,64]$ ReLU $[64,2]$	PMA(128, 4, 2, T) SAB(128, 128, 4, T) SAB(128, 128, 4, T) $[128,1]$

C.2 Hyper-parameters

Hyper-parameters used for training: $\gamma = 0.99$; policy networks are updated at the end of every episode for the same number of time steps as the episode; the time-lagged network θ_{lag} is updated every 100 training steps using $\tau = 0.2$; replay buffer size = 200000; batch size = 128; Adam optimizer is used with learning rate = $2e - 5$; ϵ -greedy is used for the first 500 time steps, where ϵ is annealed exponentially from 1.0 to 0.01. To ensure fair comparison, the hyper-parameters are the same across all four models: MLP, Deep Set, Social Attention, MIDAS.

D Results

D.1 Training Curves

Fig. 11 shows the training curves of MLP, DeepSet, SocialAttention and MIDAS.

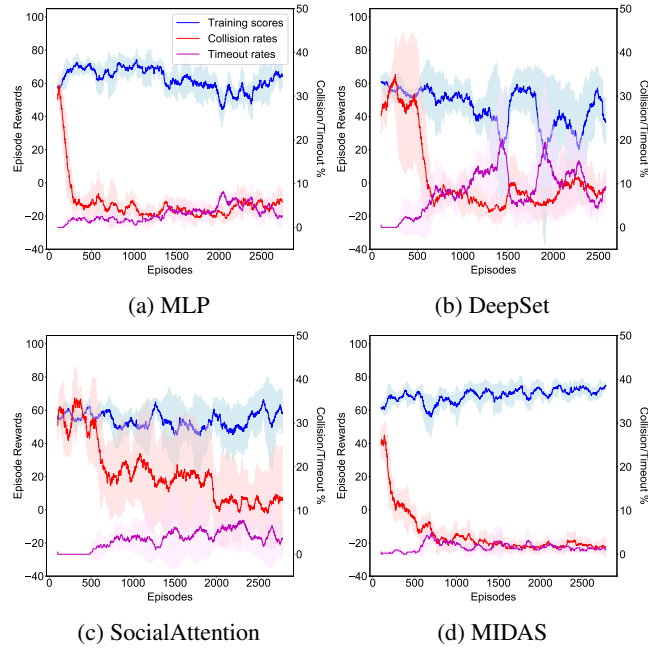


Figure 11: Training curves of the models with different attention mechanisms.

D.2 Typical Simulated Episodes

Fig. 12 and Fig. 13 show the detailed illustration of the car-following and left-turn episodes described in Sec. 4.2.

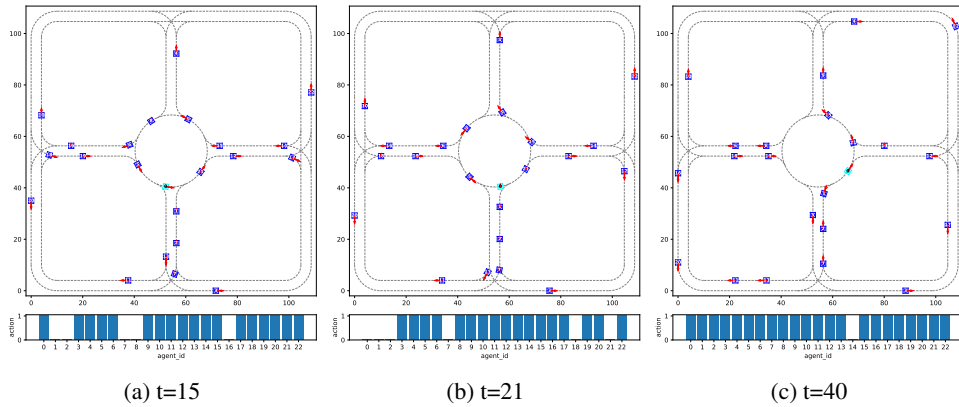


Figure 12: Illustration of Oracle and MIDAS behavior in car-following episode. Ego is cyan; all other agents are blue. At $t=15$, ego is approaching a merging point of the roundabout. At $t=21$, Oracle chooses to stop for front agent at a far distance and blocks the traffic at the intersection. MIDAS chooses to go. At $t=40$, Oracle chooses to go, since it has information about its own long-term trajectory and knows that ego will turn right. MIDAS doesn't have this information and chooses to stop and keep a distance from the front vehicle.

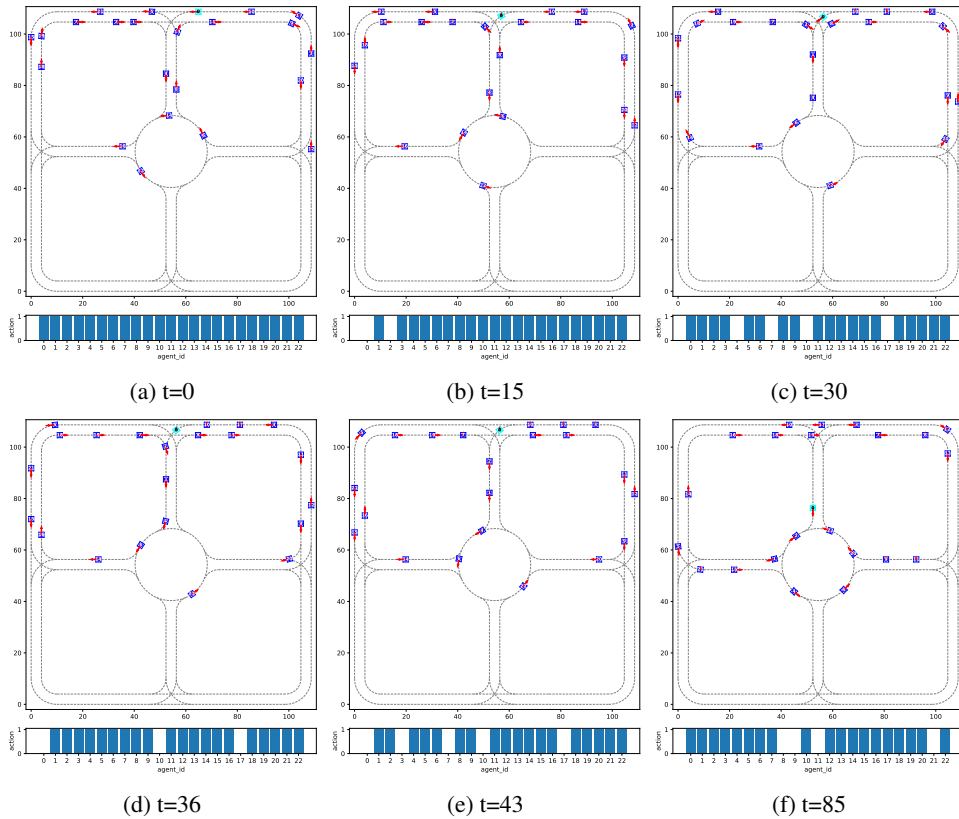


Figure 13: Illustration of Oracle and MIDAS behavior in left-turn episode. Ego is cyan; all other agents are blue. At $t=0$, ego is approaching a T-intersection. At $t=15$, ego stops for a right-turn agent. Oracle stops until $t=29$, but MIDAS chooses to go shortly after the right turn is finished. At $t=30$, Oracle wants to go, but was stopped again by a second right-turning agent. Given this state, MIDAS chooses to go at $t=36$, but Oracle waits until $t=43$ when there's a big clearance. At $t=85$, MIDAS stops for an agent in the roundabout, anticipating a right-of-way negotiation, but Oracle keeps going, given global information about tie-breaking. This episode shows that MIDAS drives more efficiently but also remains cautious at ambiguous situations, given limited information.

D.3 Model Timeout Performance across Ego Driver Types

Fig. 14 shows the change of timeout rate on the test set across different ego driver types.

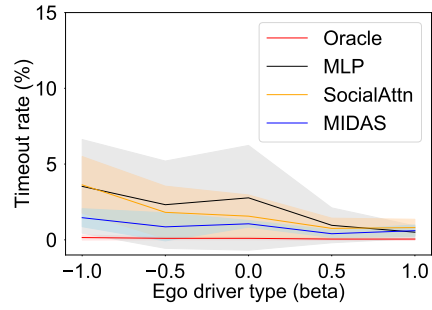


Figure 14: MIDAS has relatively constant timeout rate across different ego driver types, while that of MLP and SocialAttention decreases, accompanied with increasing collision rate, as shown in Fig. 7a. SocialAttn refers to SocialAttention.